

Oxophilicity as a Descriptor for NO Cleavage

Efficiency over Group IX Metal Clusters

Masato Yamaguchi[†], Yufei Zhang[†], Satoshi Kudoh[†], Kohei Koyama[†], Olga V. Lushchikova[‡],

Joost M. Bakker[‡] and Fumitaka Mafuné^{†}*

[†]Department of Basic Science, Graduate School of Arts and Sciences, The University of Tokyo, Komaba, Meguro-ku, Tokyo 153-8902 (Japan)

[‡]Radboud University, Institute for Molecules and Materials, FELIX laboratory, Toernooiveld 7c, 6525 ED Nijmegen (Netherlands)

AUTHOR INFORMATION

Corresponding Author

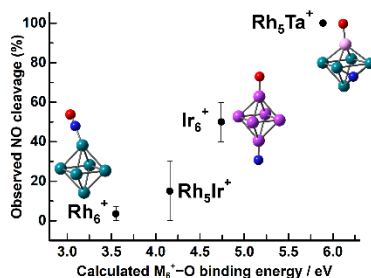
E-mail address: mafune@cluster.c.u-tokyo.ac.jp

Phone: +81-3-54546597

ABSTRACT

Iridium and rhodium are group IX elements that can both catalytically reduce NO. To understand the difference in their reactivity towards NO, the adsorption forms of NO onto clusters of Ir and Rh are compared using vibrational spectra, recorded via infrared multiple-photon dissociation spectroscopy. The spectra give evidence for the existence of at least two specific adsorption forms. The main Ir_6^+NO isomer is one in which NO is dissociated, whereas one other is a local minimum structure in the reaction pathway leading to dissociative adsorption. In contrast to adsorption onto Rh_6^+ , where less than 10% of the isomeric population was found in the global minimum associated with dissociative adsorption, a substantial fraction (about 50%) of NO dissociates on Ir_6^+ . This higher efficiency is attributed to a considerably reduced activation barrier for dissociation on Ir_6^+ . The characteristic key identified for dissociation efficiency is the cluster's affinity to atomic oxygen.

TOC GRAPHICS



KEYWORDS Oxophilicity, IRMPD, NO, Gas Phase Cluster, Geometrical Isomer

Iridium and rhodium are group IX elements, that can both catalytically reduce NO.^{1,2} As a consequence, both have been used in three-way catalytic converters in the aftertreatment system of automobiles,³ and the reaction mechanism of NO reduction over these metals has been studied intensively for a few decades. The adsorption forms of NO on extended surfaces are known to be sensitive to surface morphology and coverage: at coverages of less than 0.25 ML NO on Rh(111), adsorption is preferential on hollow (fcc) sites, but this preference shifts to on-top sites at coverages between 0.25 and 0.50 ML.⁴⁻⁷ For Ir(111) this is reversed: NO adsorbs on on-top sites at low coverage and only populates hollow sites at higher coverage.⁸ In addition, on planar Ir(210) NO adsorbs on on-top sites, whereas on faceted Ir (210) it occupies bridge and on-top sites. Faceted Ir(210) has been demonstrated to be active toward NO decomposition even under 0.70 ML coverage by O atoms.⁹

As the reaction efficiency sensitively varies with reaction conditions, the use of a gas-phase cluster to investigate the largely unknown reaction mechanism can be very instructive, because clusters and molecules involved in the reaction can be probed with atomic detail using mass spectrometry.¹⁰⁻¹⁴ Moreover, the combination with infrared (IR) spectroscopy allows structure determination of (intermediate) adsorption products allowing for the validation of proposed reaction mechanisms.

Recently, we elucidated the adsorption form of NO on cationic Rh clusters, Rh_n^+ ($n = 6-16$), using IR multiple-photon dissociation (IRMPD) spectroscopy combined with density functional theory (DFT) calculations.¹⁵⁻¹⁹ The spectra show that NO molecules predominantly adsorb on on-top sites of Rh_n^+ for all n studied, and that only a small fraction of NO adsorbs dissociatively

on Rh_n^+ , with the precise ratio of dissociative to molecular adsorption depending on the cluster size n . For Rh_6^+ , almost all NO adsorbs molecularly on the on-top site of the Rh_6^+ octahedron. Although the DFT calculations predict that dissociative adsorption of NO is thermodynamically favored over molecular (intact) adsorption for Rh_6^+ , they also show that this is kinetically hindered by the activation barrier for NO cleavage, corroborating the rather low observed NO dissociation.

To understand what is the main factor that causes the relative height of this barrier, we here investigate the adsorption of NO on a cluster of a second group IX element. We probe the structure of Ir_6^+NO using IR photodissociation spectroscopy of complexes with Ar, $\text{Ir}_6^+\text{NO-Ar}_m$, and observe the release of Ar atoms as a probe of vibrational excitation. Figure 1 shows the IRMPD spectrum for $\text{Ir}_6^+\text{NO-Ar}_m$ (panel a) and calculated spectra of three stable isomers (panels b-d), of which two exhibit separate binding of N and O atoms to Ir_6^+ , and only one has NO as an intact molecule. The most stable isomer A (panel b), is an octahedral Ir_6^+ cluster with the N and O atoms on opposite on-top sites. Two other stable isomers are prismatic Ir_6^+ clusters with molecular NO on an on-top site (isomer B, panel c), or with the O atom on an on-top site and the N atom on a bridge site, respectively (isomer C, panel d).

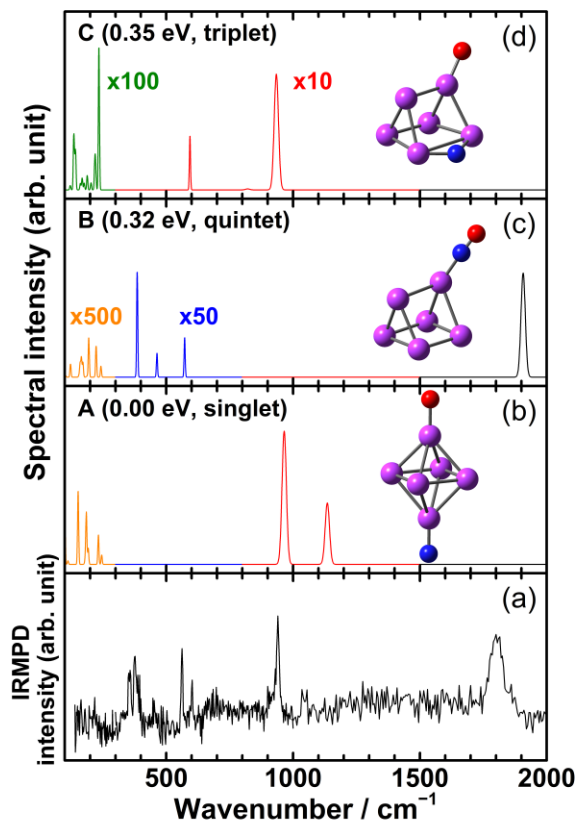


Figure 1. (a) IRMPD spectrum for $\text{Ir}_6^+ \text{NO-Ar}$ and (b–d) DFT calculated vibrational spectra of the stable isomers of $\text{Ir}_6^+ \text{NO}$. The relative energy of formation and spin multiplicity are shown in parentheses for each structure. Blue, red, and purple balls represent N, O, and Ir atoms, respectively (see Figure S2 for other isomers).

The experimental IRMPD spectrum is dominated by relatively strong bands at 355, 375, 563, 940, and 1805 cm^{-1} , with weaker bands at 450, 603, and 1045 cm^{-1} . The 1805 cm^{-1} band is substantially broader than the lower frequency bands, even taking into account the larger spectral bandwidth of the IR laser at higher frequencies (approx. 0.5% of the central frequency FWHM); it thus appears likely that this band is saturated. A band observed at this frequency is

characteristic for an intact NO molecule through its stretching vibration: for NO adsorbed on an on-top site of Ir(111) this frequency is 1860 cm^{-1} .²⁰ As shown in Figure 1(c), isomer B contains an intact NO molecule and exhibits a strong band around 1900 cm^{-1} . The maximum depletion observed for this band is 40-50%, suggesting that this is due to only one of multiple isomers present in the beam, and that the other isomers carry no intact NO, and consequently do not lose Ar at these frequencies. This experimental band thus indicates that at least a fraction of the population sampled has NO molecularly adsorbed on Ir_6^+ . Consistent with this, the predicted vibrational spectrum of isomer B exhibits no bands in the $600\text{--}1800\text{ cm}^{-1}$ spectral region, so this isomer alone cannot explain the pronounced band at 940 cm^{-1} and the weaker band at 1045 cm^{-1} observed experimentally. In contrast, bands at such frequencies are predicted for isomer A with O and N atoms adsorbed separately on on-top sites; calculated at 980 and 1130 cm^{-1} , respectively, they correspond to stretching vibrations of the terminal O and N atoms, respectively. The bands observed at 563 , 450 , and 355 or 375 cm^{-1} are consistent with isomer B. Thus, the IRMPD spectrum agrees favorably with a combination of vibrational spectra of isomers A and B, leaving only the bands at 603 and 355 or 375 cm^{-1} unaccounted for. These two bands are likely due to one or more further isomers, of which we found a large number (cf. Figure S2), and one of these is isomer C. Other prismatic Ir_6^+ isomers with the O atom on the on-top site and the N atom on a different bridge site could be possible, but they typically exhibit a band or bands at $>620\text{ cm}^{-1}$ (see Figure S2). In summary, we conclude that the spectrum is due to the co-existence of three structural isomers, with both molecular and dissociative adsorption present.

If we assume that the band intensity in the IRMPD spectrum is proportional to the product of the calculated vibrational band spectral intensity and the relative isomeric population, the latter can be estimated to be approximately 25% and 60% for isomers A and B, respectively,

with a possible further 15% for a third isomer, for instance isomer C. This estimate is consistent with the observed depletion on the order of 40–50 % at 1805 cm^{-1} .

The question arises whether the presence of these isomers can be rationalized based on a possible reaction pathway. Figure 2 shows a reactive potential energy surface (PES) for the adsorption and subsequent dissociation of NO on Ir_6^+ on the quintet PES. For Ir_6^+ , we found a prism to be the global minimum structure with sextet multiplicity. Since isomer B, one of the lowest energy prismatic Ir_6^+ isomers with NO molecularly adsorbed, is found on the quintet surface, we restricted our reaction pathway search to this surface. The NO molecule initially adsorbs on an on-top site of Ir_6^+ through the N atom with a binding energy of 2.32 eV (IM1). This orientation is common to small, N-containing molecules on metal surfaces.^{21,22} After adsorption, the NO molecule leans towards a neighboring Ir atom until the O atom is bound to it (IM2). The NO bond is ruptured after passing TS2, forming separately adsorbed O and N atoms (IM3). The N atom then migrates to the next Ir atom via a bridge site (IM4) to end up as a terminal N (IM5). Finally, Ir_6^+ transforms from prism to octahedron (P). The whole reaction path is downhill, and all barriers are below the energy of the reactants (R), thus the reaction is kinetically favored. However, as the internal energy of the cluster can be dissipated by thermalizing collisions with the surrounding carrier gas atoms during the reaction, each transition state can be a barrier which halts the successive reaction step, leaving population in the intermediate state. Indeed, isomers B and C correspond to intermediates IM1 and IM4 respectively, en route to the final product A. The highest barrier, TS2, is 0.26 eV below R; More than a half of the clusters were not able to cross this barrier and were observed as isomer B.

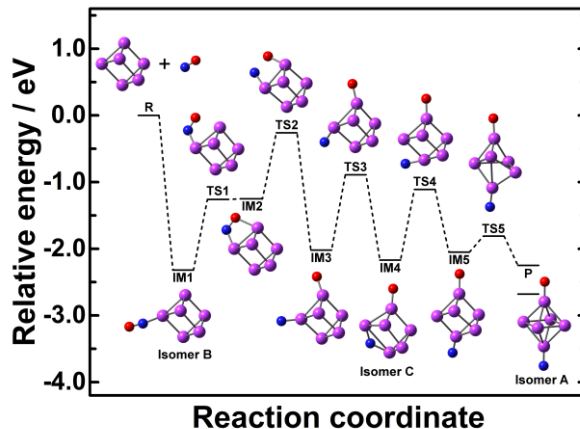


Figure 2. Reaction pathway for NO dissociation on Ir_6^+ , calculated on the quintet spin surface. R, IM, TS and P indicate reactant, intermediate, transition state, and product, respectively. The most stable spin isomer of P (singlet) is also shown. Geometries of IM1, IM4 and P correspond to isomers B, C and A in Figure 1, respectively.

The found fraction of at least 50% isomers with NO dissociated (A and C) for Ir_6^+ , is in stark contrast with Rh_6^+ where molecularly adsorbed NO is strongly dominant.¹⁵ To understand this difference, we first compare the calculated reactive PESs. The reactive PES for NO dissociation over Rh_6^+ was found to be quite similar to that for Ir_6^+ :²³ After on-top adsorption of NO on Rh_6^+ , the NO molecule migrates to a bridge site, leaning toward a Rh atom until the O atom binds to it. However, the transition state for bond cleavage on Rh_6^+ is located 0.7 eV *higher* than the reactants. This activation barrier thus prevents NO dissociation over Rh_6^+ . In contrast, for Rh_5Ta^+ , on which NO was observed to dissociate with near-unity efficiency, the transition state for bond cleavage is located 1.1 eV *lower* than the reactants. Thus, the activation barrier for bond cleavage, where the O is abstracted towards another metal atom, is critically important for dissociation of NO, and its relative height appears to be decisive for successful NO cleavage.

But what then underlies these relative barrier heights? For this, we examine the structural preferences for adsorption. We first note that the global minima, where NO is dissociatively bound to Rh_6^+ and Ir_6^+ , respectively, are markedly distinct: where for Ir_6^+ both N and O are adsorbed on on-top sites (evidenced by the experimental band at 940 cm^{-1}), for Rh_6^+ both are located on hollow sites. This preference seems reflected in the transition state structures for both species (Figure 3) when NO undergoes bond cleavage: for Ir_6^+ , N-bound on-top adsorption is retained even in the transition state structure, forming an Ir-N-O-Ir chain structure. On Rh_6^+ , the N cannot retain its position on a hollow site, but still prefers bridge adsorption in the transition state. This propensity for Rh_6^+ to bind N on a bridge motif is seen throughout the reactive PES, with the exception of the entrance complex;¹² Ir exhibits on-top binding throughout the reaction pathway. These findings strongly correlate to the experimental findings for the low-coverage regime on (111) surfaces of Rh and Ir.⁴ From this, we conclude that the adsorption of NO onto clusters is essentially the same as for the bulk, thereby establishing clusters as a useful model system for the adsorption, and potentially for the reduction reaction.

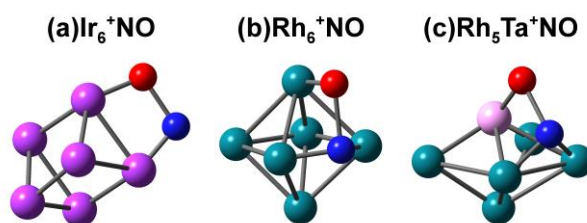


Figure 3. Geometrical structures of (a) Ir_6^+NO (b) Rh_6^+NO and (c) $\text{Rh}_5\text{Ta}^+\text{NO}$ in the transition state for bond cleavage.

Close examination of the orbitals obtained by the calculations suggests that d-orbitals of the Ir atom interact with the π orbitals of NO (see Figure S3). In addition, separate N and O atoms

can stably adsorb on on-top sites of the Ir cluster. This is also found computationally by Zhou *et al.*, who report that up to three O atoms adsorb on-top on pyramidal Ir_5^+ .²⁴ The propensity of on-top adsorption is further reflected in the relatively high energy of formation of an isomer with O and N atoms on bridge sites of Ir_6^+ (+0.71 eV).

However, the key binding preference is not that for N, but for O. The structural characteristic common to all three transition states shown in Figure 3 is that the O binds to a neighboring on-top site. In a series of experiments, we obtained the propensities for NO dissociative adsorption on Rh_6^+ , Rh_5Ta^+ , and Ir_6^+ . The found propensities exhibit a strong correlation with the oxygen affinities of the clusters as illustrated, whereas the affinities towards nitrogen are essentially identical (see Figure 4). This finding indicates that we are able to predict the NO dissociation efficiency by evaluating the oxygen-atom adsorption energies. This forms a crucial refinement of work by Sakaki and coworkers, who conclude that dissociation is preferred by metals with strong N- and O-affinities (Ru_n and Rh_n in particular).²⁵ Here, we conclude that N-affinity facilitates adsorption, whereas it is the O-affinity that governs dissociation efficiency.

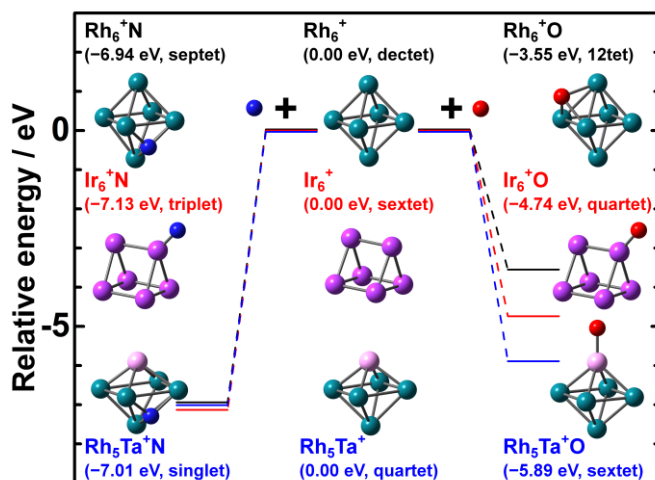


Figure 4. N- and O-atom affinities of the metal cationic clusters.

In conclusion, we find that the adsorption on Ir and Rh clusters shows great similarities with equivalent process on extended surfaces. From the found dissociation propensities upon adsorption onto clusters with different elemental compositions, we conclude that the oxophilicity of the adsorption site forms a descriptor for the NO cleavage reaction efficiency. Although optimizing catalysts for the overall NO reduction reaction will certainly require more descriptors, we expect that employing the oxophilicity of adsorption sites will become an important figure of merit for the design of tailored NO reduction catalysts.

ASSOCIATED CONTENT

Supporting Information

Supporting Information is available.

File type: PDF

The following file is available free of charge.

AUTHOR INFORMATION

Notes

The authors declare no competing financial interests.

ACKNOWLEDGMENT

We gratefully acknowledge the Nederlandse Organisatie voor Wetenschappelijk Onderzoek (NWO) for the support of the FELIX Laboratory, and thank the FELIX staff, particularly Dr. Britta Redlich for her skillful assistance. This work was supported in part by JSPS KAKENHI, Grant-in-Aid for JSPS Fellows (no. JP18J21934). We used supercomputers at the Research Center for Computational Science, Okazaki Research Facilities, National Institutes of Natural Sciences.

REFERENCES

- (1) Kašpar, J.; Fornasiero, P.; Hickey, N. Automotive Catalytic Converters: Current Status and Some Perspectives. *Catal. Today* 2003, 77 (4), 419–449, [https://doi.org/10.1016/S0920-5861\(02\)00384-X](https://doi.org/10.1016/S0920-5861(02)00384-X).
- (2) Shimokawabe, M.; Umeda, N. Selective Catalytic Reduction of NO by CO over Supported Iridium and Rhodium Catalysts. *Chem. Lett.* 2004, 33 (5), 534–535, <https://doi.org/10.1246/cl.2004.534>.
- (3) Nieuwenhuys, B. E. The Surface Science Approach Toward Understanding Automotive Exhaust Conversion Catalysis at the Atomic Level. *Adv. Catal.* 1999, 44, 259–328, [https://doi.org/10.1016/S0360-0564\(08\)60514-3](https://doi.org/10.1016/S0360-0564(08)60514-3).
- (4) Zasada, I.; Van Hove, M. .; Somorjai, G. . Reanalysis of the Rh(111)+(2×2)-3NO Structure Using Automated Tensor LEED. *Surf. Sci.* 1998, 418 (3), L89–L93, [https://doi.org/10.1016/S0039-6028\(98\)00782-1](https://doi.org/10.1016/S0039-6028(98)00782-1).

- (5) Kim, Y. J.; Thevuthasan, S.; Herman, G. S.; Peden, C. H. F.; Chambers, S. A.; Belton, D. N.; Permana, H. Chemisorption Geometry of NO on Rh(111) by X-Ray Photoelectron Diffraction. *Surf. Sci.* 1996, 359 (1–3), 269–279, [https://doi.org/10.1016/0039-6028\(96\)00027-1](https://doi.org/10.1016/0039-6028(96)00027-1).
- (6) Nakamura, I.; Kobayashi, Y.; Hamada, H.; Fujitani, T. Adsorption Behavior and Reaction Properties of NO and CO on Rh(1 1 1). *Surf. Sci.* 2006, 600 (16), 3235–3242, <https://doi.org/10.1016/J.SUSC.2006.06.009>.
- (7) Wallace, W. T.; Cai, Y.; Chen, M. S.; Goodman, D. W. NO Adsorption and Dissociation on Rh(111): PM-IRAS Study. *J. Phys. Chem. B* 2006, 110 (12), 6245–6249, <https://doi.org/10.1021/jp057134p>.
- (8) Fujitani, T.; Nakamura, I.; Kobayashi, Y.; Takahashi, A.; Haneda, M.; Hamada, H. Adsorption and Reactions of NO on Clean and CO-Precovered Ir(111). *J. Phys. Chem. B* 2005, 109, 17603–17607, <https://doi.org/10.1021/JP053092T>.
- (9) Chen, W.; Stottlemeyer, A. L.; Chen, J. G.; Kaghazchi, P.; Jacob, T.; Madey, T. E.; Bartynski, R. A. Adsorption and Decomposition of NO on O-Covered Planar and Faceted Ir(2 1 0). *Surf. Sci.* 2009, 603 (20), 3136–3144, <https://doi.org/10.1016/J.SUSC.2009.08.027>.
- (10) Johnson, G. E.; Mitrić, R.; Bonačić-Koutecký, V.; Castleman, A. W. Clusters as Model Systems for Investigating Nanoscale Oxidation Catalysis. *Chem. Phys. Lett.* 2009, 475 (1–3), 1–9, <https://doi.org/10.1016/J.CPLETT.2009.04.003>.
- (11) Lang, S. M.; Bernhardt, T. M. Gas Phase Metal Cluster Model Systems for Heterogeneous Catalysis. *Phys. Chem. Chem. Phys.* 2012, 14 (26), 9255–9269, <https://doi.org/10.1039/c2cp40660h>.

(12) Tawarayaya, Y.; Kudoh, S.; Miyajima, K.; Mafuné, F. Thermal Desorption and Reaction of NO Adsorbed on Rhodium Cluster Ions Studied by Thermal Desorption Spectroscopy. *J. Phys. Chem. A* 2015, 119 (31), 8461–8468, <https://doi.org/10.1021/acs.jpca.5b04224>.

(13) Anderson, M. L.; Ford, M. S.; Derrick, P. J.; Drewello, T.; Woodruff, D. P.; Mackenzie, S. R. Nitric Oxide Decomposition on Small Rhodium Clusters, $\text{Rh}_n^{+/-}$. *J. Phys. Chem. A* 2006, 110 (38), 10992–11000, <https://doi.org/10.1021/jp062178z>.

(14) Hirabayashi, S.; Ichihashi, M. Effects of Second-Metal (Al, V, Co) Doping on the NO Reactivity of Small Rhodium Cluster Cations. *J. Phys. Chem. A* 2017, 121 (13), 2545–2551, <https://doi.org/10.1021/acs.jpca.6b11613>.

(15) Nagata, T.; Koyama, K.; Kudoh, S.; Miyajima, K.; Bakker, J. M.; Mafune, F. Adsorption Forms of NO on Rh_n^+ ($n = 6-16$) Revealed by Infrared Multiple Photon Dissociation Spectroscopy. *J. Phys. Chem. C* 2017, 121 (49), 27417–27426, <https://doi.org/10.1021/acs.jpcc.7b08097>.

(16) Nagata, T.; Kudoh, S.; Miyajima, K.; Bakker, J. M.; Mafuné, F. Adsorption of Multiple NO Molecules on Rh_n^+ ($n = 6, 7$) Investigated by Infrared Multiple Photon Dissociation Spectroscopy. *J. Phys. Chem. C* 2018, 122 (40), 22884–22891, <https://doi.org/10.1021/acs.jpcc.8b04729>.

(17) Hermes, A. C.; Hamilton, S. M.; Hopkins, W. S.; Harding, D. J.; Kerpál, C.; Meijer, G.; Fielicke, A.; Mackenzie, S. R. Effects of Coadsorbed Oxygen on the Infrared Driven Decomposition of N_2O on Isolated Rh_5^+ Clusters. *J. Phys. Chem. Lett.* 2011, 2 (24), 3053–3057, <https://doi.org/10.1021/jz2012963>.

(18) Hamilton, S. M.; Hopkins, W. S.; Harding, D. J.; Walsh, T. R.; Gruene, P.; Haertelt, M.; Fielicke, A.; Meijer, G.; Mackenzie, S. R. Infrared Induced Reactivity on the Surface of Isolated Size-Selected Clusters: Dissociation of N₂O on Rhodium Clusters. *J. Am. Chem. Soc.* 2010, 132 (5), 1448–1449, <https://doi.org/10.1021/ja907496c>.

(19) Frisch, M. J.; Trucks, G. W.; Schlegel, H. B.; Scuseria, G. E.; Robb, M. A.; Cheeseman, J. R.; Scalmani, G.; Barone, V.; Mennucci, B.; Petersson, G. A.; Nakatsuji, H.; CT, W.; et al. Gaussian 09, Revision E.01. Gaussian 09 2013.

(20) Cornish, J. C. L.; Avery, N. R. Adsorption of N₂, O₂, N₂O and NO on Ir(111) by EELS and TPD. *Surf. Sci.* 1990, 235 (2–3), 209–216, [https://doi.org/10.1016/0039-6028\(90\)90795-A](https://doi.org/10.1016/0039-6028(90)90795-A).

(21) Zeigarnik, A. V. Adsorption and Reactions of N₂O on Transition Metal Surfaces. *Kinet. Catal.* 2003, 44 (2), 233–246, <https://doi.org/10.1023/A:1023308629868>.

(22) Watanabe, K.; Kokalj, A.; Horino, H.; Rzeznicka, I. I.; Takahashi, K.; Nishi, N.; Matsushima, T. Scanning-Tunneling Microscopy, Near-Edge X-Ray-Absorption Fine Structure, and Density-Functional Theory Studies of N₂O Orientation on Pd(110). *Jpn. J. Appl. Phys.* 2006, 45 (3B), 2290–2294, <https://doi.org/10.1143/JJAP.45.2290>.

(23) Yamaguchi, M.; Kudoh, S.; Miyajima, K.; Lushchikova, O. V.; Bakker, J. M.; Mafuné, F. Tuning the Dissociative Action of Cationic Rh Clusters Toward NO by Substituting a Single Ta Atom. *J. Phys. Chem. C* 2019, 123 (6), 3476–3481, <https://doi.org/10.1021/acs.jpcc.8b08575>.

(24) Zhou, X.; Yang, J.; Li, C. Theoretical Study of Structure, Stability, and the Hydrolysis Reactions of Small Iridium Oxide Nanoclusters. *J. Phys. Chem. A* 2012, 116 (40), 9985–9995, <https://doi.org/10.1021/jp3064068>.

(25) Takagi, N.; Ishimura, K.; Fukuda, R.; Ehara, M.; Sakaki, S. Reaction Behavior of the NO Molecule on the Surface of an M_n Particle ($M = \text{Ru, Rh, Pd, and Ag; } n = 13 \text{ and } 55$): Theoretical Study of Its Dependence on Transition-Metal Element. *J. Phys. Chem. A* 2019, 123 (32), 7021–7033, <https://doi.org/10.1021/acs.jpca.9b04069>.